Classification
Physics Abstracts
61.30 — 42.00 — 42.20

Transmission and reflection of a monochromatic beam in a twisted nematic wedge

S. Faetti ([1, 2]), M. Nobili ([1, 2]) and I. Raggi ([1])

([1]) Dipartimento di Fisica, Università di Pisa, Piazza Torricelli 2, 56100 Pisa, Italy
([2]) Consorzio Nazionale interuniversitario di Fisica della Materia and Gruppo Nazionale di Struttura della Materia del Consiglio Nazionale delle Ricerche

(Received 12 August 1993, received in final form 18 October 1993, accepted 2 November 1993)

Abstract. — The transmission and reflection of a monochromatic electromagnetic wave in a twisted nematic wedge are investigated. We consider the special case where the characteristic length ξ of the director twist is much higher than the optical wavelength λ. By using the perturbative theoretical procedure proposed by Oldano *et al.*, we find an analytic expression for the transmitted and reflected beams at the first order in the perturbative parameter $\varepsilon = 1/\Delta k\xi$, where Δk is the difference between the extraordinary and ordinary wavenumbers. The intensity and the polarization of the refracted and reflected beams are related by simple analytic expressions to the normal derivatives of the director at the interfaces and do not depend on details of the bulk director distortion. The theoretical predictions are compared with experimental results obtained using an electric field to twist the director-field. A satisfactory agreement is found between theory and experiment. On the basis of our theoretical results we propose a simple experimental method to measure the twist viscosity coefficient of nematic liquid crystals.

1. Introduction.

Nematic liquid crystals (NLC) are uniaxial anisotropic media whose optical axis is usually represented by a unit vector **n** called « *the director* ». The director orientation is strongly affected by interactions with the boundary walls and with external fields such as electric or magnetic fields. The great sensitivity of **n** to external fields makes NLC very interesting media for electrooptic and magnetooptic applications. For this reason a great number of theoretical and experimental papers have been published on the optical properties of non-homogeneous uniaxial media [1-17]. We report here on the special case of a twisted nematic cell where the director-field lies parallel to the $x - y$ plane and makes the azimuthal angle $\varphi(z)$ with the easy-axis. We are interested in investigating the optical properties of a wedge NLC sample from both the theoretical and experimental points of view in the case where the characteristic length ξ of the director twist-distortion is much higher than the optical wavelength λ of the electromagnetic beam. By using the perturbative procedure proposed some years ago by

Oldano *et al.* [9, 10, 16] for a stratified planar NLC layer, we will show that a very simple analytic expression can be obtained at the first order in the perturbation parameter $\varepsilon = 1/\Delta k\xi$, where Δk is the difference between the extraordinary and ordinary wavenumbers. This expression does not depend on details of the director distortion but only on the values of the derivatives $\partial\varphi/\partial z$ at the interfaces of the NLC sample. The results predicted by this theoretical approach allow a simple physical interpretation, and they are used to describe the propagation of an electromagnetic monochromatic wave in a wedge NLC cell. As a main result of our approach we are able to show that, due to the breaking of the well-known adiabatic theorem, the NLC cell separates the incident beam into two refracted beams at two refraction angles corresponding to the ordinary and the extraordinary refractive indices. The electromagnetic beams that are reflected by the last interface of the NLC wedge cell are always separated into three different refracted beams. The deflection angles of two of these beams correspond to the ordinary and extraordinary optical beams propagating in a homogeneous planar NLC wedge, whilst the deflection angle of the third beam is exactly intermediate between the other two. This means that the third beam « sees » an average index

$$n_A = (n_e + n_o)/2 ,$$

where n_e and n_o are the extraordinary and the ordinary indices, respectively. In the following sections we will denote this beam as « *the non-adiabatic reflected beam* ». The intensity of this reflected beam is poorly dependent on the polarization of the incident beam and proportional to $(\partial\varphi/\partial z)^2$ at the two interfaces of the NLC. Its polarization plane is found to be perpendicular to that of the incident beam if the polarization of the incident beam is parallel (or orthogonal) to the director orientation at the first interface.

The subsection 2.1 is devoted to the theoretical analysis of the propagation of an electromagnetic beam in a twisted NLC by using the perturbative procedure given in references [9, 10, 16]. In subsection 2.2 this approach is generalized for a twisted NLC wedge. In section 2.3 the static and dynamic features of the twist distortion induced by an electric field are discussed. In subsection 3.1 we describe the experimental apparatus and the experimental procedure. Subsection 3.2 is devoted to the experimental results and to their comparison with the theoretical predictions. By exploiting our theoretical results, we propose a simple experimental method to measure the twist viscosity coefficient γ of nematic liquid crystals.

2. Transmission and reflection properties of a twisted NLC.

2.1 TRANSMISSION AND REFLECTION BY A TWISTED PLANAR NEMATIC LAYER. — We start our discussion by considering the simplest case of a planar NLC layer of thickness d sandwiched between two glass plates of thicknesses d_1 and d_2 as shown in figure 1. The origin of the orthogonal frame is chosen at the centre of the layer and the z-axis is orthogonal to the layer. The director easy alignment $\mathbf{n}_0$ at the two interfaces is at an angle β with respect to the x-axis in the x-y plane. If a magnetic (or electric) field is applied in the film plane along the x-axis, a director twist $\varphi(z)$ occurs in the NLC layer. $\varphi(z)$ denotes the angle between director $\mathbf{n}(z)$ and easy axis $\mathbf{n}_0$. We denote by φ_1 and φ_2 the director angles at the glass-nematic interface 1 ($z = -d/2$) and at the nematic-glass interface 2 ($z = +d/2$), respectively (see Fig. 1). A monochromatic plane wave of wavelength λ impinges at a normal incidence on the system. The propagation of the electromagnetic field in the NLC layer can be obtained by using the Berreman [12] theoretical procedure. The electromagnetic field at a given point z is related to that at another point z_0 by the Berreman 4×4 propagation matrix $\bar{\bar{J}}(z_0, z)$ defined by :

$$\psi(z) = \bar{\bar{J}}(z_0, z)\,\psi(z_0) , \tag{2.1}$$

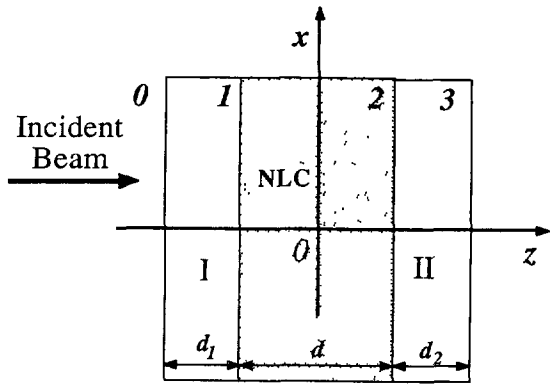

Fig. 1. — Geometry of the planar NLC layer. The NLC of thickness d is sandwiched between two glass plates I and II of thickness d_1 and d_2. A monochromatic electromagnetic beam impinges at normal incidence on the NLC layer. The numbers 0, 1, 2, 3 denote the four interfaces of the system.

where $\psi(z)$ represents a four dimension vector $[E_x, H_y, E_y, -H_x]$ and E_x, E_y, H_x, H_y are the x and y-components of the electric and magnetic fields of the electromagnetic wave. In general, the propagation matrix can only be calculated by using numerical methods ; however much simpler expressions can be obtained if the characteristic length ξ of the director distortion is much greater than the optical wavelength λ. In this section we follow the perturbative analysis of Oldano *et al.* [9, 10, 16]. The first step consists of using a special base made of four vectors which correspond to two progressive and two regressive waves. These waves represent the progressive and regressive extraordinary and ordinary waves having the electric field parallel and orthogonal to the **local** orientation of **n**, respectively. The wavenumbers of the extraordinary and ordinary waves are $k_e = 2\pi n_e/\lambda$ and $k_o = 2\pi n_o/\lambda$, respectively. An important parameter of the theory is wavenumber anisotropy $\Delta k = k_e - k_o$. For $\lambda \ll \xi$, the coupling between progressive and regressive waves is very small and can be disregarded [10]. Therefore we can analyse, separately, the propagation of the progressive and regressive electromagnetic waves using a 2×2 Jones matrix in the subset base made by the two progressive (or regressive) ordinary and extraordinary waves. The electric field of the base follows the local rotation of the director-field. The electromagnetic field of the progressive waves at a given point z is, then, related to that at the point z_0 by a 2×2 transmission matrix $\bar{\bar{T}}_P(z_0, z)$ that is defined by :

$$\mathbf{\Phi}(z) = \bar{\bar{T}}_P(z_0, z)\, \mathbf{\Phi}(z_0)\,, \tag{2.2}$$

with

$$\mathbf{\Phi} = \begin{vmatrix} e^+ \\ o^+ \end{vmatrix}, \tag{2.3}$$

where e^+ and o^+ are the amplitudes of the progressive extraordinary and ordinary wave, respectively. e^- and o^+ correspond to the components of the electric field respectively parallel and orthogonal to **n**. An analogous equation can be written for the regressive waves by defining a regressive transmission matrix $\bar{\bar{T}}_R(z_0, z)$. According to Oldano *et al.*, a perturbative expansion of $\bar{\bar{T}}_P(z_0, z)$ can be obtained in the small parameter $\varepsilon = 1/\Delta k\xi$. At the first order in ε

they found [16] :

$$\bar{\bar{T}}_P = \bar{\bar{T}}_P\left(-\frac{d}{2}, \frac{d}{2}\right) = \exp(ik_A d)\begin{vmatrix} \exp\left(i\frac{\delta}{2}\right) & it \\ it^* & \exp\left(-i\frac{\delta}{2}\right) \end{vmatrix}, \tag{2.4}$$

with

$$t = -i\eta_1 \int_{-\frac{d}{2}}^{\frac{d}{2}} \exp(i\,\Delta kz)\frac{\partial\varphi}{\partial z}\,dz\,, \tag{2.5}$$

where $\eta_1 = (\sqrt{n_e/n_o} + \sqrt{n_o/n_e})/2$; $k_A = (k_e + k_o)/2$; $\Delta k = k_e - k_o$ and $\delta = \Delta k d$. For a typical NLC sample as 5CB, the refractive indices are $n_e \approx 1.7$, $n_o \approx 1.53$ and, thus, $\eta_1 \approx 1.0014$. The role of contributions of higher order in ε has been investigated in reference [17].

Equations (2.4) and (2.5) have been obtained by disregarding contributions of orders higher than the first order in the small parameter ε. Accordingly, we can calculate the integral in (2.5) at the same order of approximation. By successive integrations by parts we easily find :

$$t = -\frac{\eta_1}{\Delta k}\left\{\left|\frac{\partial\varphi}{\partial z}\exp(+\,i\,\Delta kz)\right|_{-\frac{d}{2}}^{\frac{d}{2}} - \frac{i}{\Delta k}\left|\frac{\partial^2\varphi}{\partial z^2}\exp(+\,i\,\Delta kz)\right|_{-\frac{d}{2}}^{\frac{d}{2}} + \cdot\right\}. \tag{2.6}$$

Since $\partial\varphi/\partial z \approx \Delta\varphi/\xi$ and $\partial^2\varphi/\partial z^2 \approx \Delta\varphi/\xi^2$, all terms in the right side end of (2.6), except the first term, are of an order higher than the first order in ε and, thus, can be disregarded. Therefore the coefficient t becomes :

$$t = -\frac{\eta_1}{\Delta k}\left[\frac{\partial\varphi(d/2)}{\partial z}\exp\left(+\,i\,\frac{\delta}{2}\right) - \frac{\partial\varphi(-\,d/2)}{\partial z}\exp\left(-\,i\,\frac{\delta}{2}\right)\right]. \tag{2.7}$$

At the first order in ε, t is proportional to $\partial\varphi/\partial z$ at the interfaces of the NLC layer and does not depend on details of the bulk director distortion. Furthermore, as will be shown below, the analytic expression in (2.7) allows us to obtain a simple physical interpretation of the main mechanisms connected with the propagation of an electromagnetic wave in a twisted NLC. If the director twist is generated by a magnetic (or an electric) field with characteristic distortion thickness $\xi \ll d$, we can show [see Sect. 2.3] that the director derivatives at the two glass-nematic interfaces are given by :

$$\frac{\partial\varphi\left(-\frac{d}{2}\right)}{\partial z} = \frac{\sin(\beta - \varphi_1)}{\xi} \quad \text{and} \quad \frac{\partial\varphi\left(\frac{d}{2}\right)}{\partial z} = -\frac{\sin(\beta - \varphi_2)}{\xi}, \tag{2.8}$$

with $\beta > \varphi_1$ and $\beta > \varphi_2$ and where ξ is the magnetic (or electric) coherence length. By substituting (2.8) in (2.7) and (2.4) we finally obtain :

$$\bar{\bar{T}}_P = \begin{vmatrix} \exp(ik_e d) & i[a\exp(ik_e d) + b\exp(ik_o d)] \\ i[b\exp(ik_e d) + a\exp(ik_o d)] & \exp(ik_o d) \end{vmatrix}, \tag{2.9}$$

where

$$a = \frac{\eta_1}{\Delta k\xi}\sin(\beta - \varphi_2) \quad \text{and} \quad b = \frac{\eta_1}{\Delta k\xi}\sin(\beta - \varphi_1)\,. \tag{2.9'}$$

a and b in (2.9′) are proportional to $\varepsilon = 1/\Delta k\xi$. $\bar{\bar{T}}_P$ describes the propagation of a progressive electromagnetic wave from the first glass-nematic interface 1 to the second nematic-glass interface 2. A similar matrix can be obtained for regressive waves going from the second interface 2 to the first interface 1. The transmission matrix $\bar{\bar{T}}_R = \bar{\bar{T}}_R\left(\frac{d}{2}, -\frac{d}{2}\right)$ for these regressive waves has the same form of (2.9) with a and b exchanged.

To fully describe the behaviour of an incident beam which passes through the glass plates and the NLC layer one should take into account the energy losses due to reflections at the air-glass and glass-nematic interfaces and the light diffusion due to thermal director fluctuations in the NLC [18]. In this paper, as far as the transmission properties of optical beams are concerned, we will disregard these small effects by assuming unitary transmission coefficients at these interfaces. We denote now by $\mathbf{E}^i$ the electric field of the incident beam just before the first air-glass interface 0 ($z = z_1 = -d_1 - d/2$) (see Fig. 2); by $\mathbf{E}^t$ the electric field of the transmitted beam just after the second glass-air interface 3 ($z = z_2 = d_2 + d/2$); by $\mathbf{E}^r$ the electric field of the electromagnetic wave which passes through the NLC layer is reflected at the second glass-air interface returning then at the starting point $z = z_1$. Note that, in the planar NLC layer, there are other beams that are reflected by the other interfaces and contribute to the total reflected electric field. However, as shown in section 2.2, these different reflected beams can be easily separated if the nematic cell has a wedge shape. Therefore we can here consider only the optical beams which are reflected by the second glass-air interface. According to our previous analysis $\mathbf{E}^i$ and $\mathbf{E}^r$ must be written with respect to the axes $\mathbf{n}$ and $\mathbf{h}$ where $\mathbf{n}$ is the director at the first glass-nematic interface and $\mathbf{h}$ is a unit vector orthogonal to the director. $\mathbf{E}^t$ is written with respect to the corresponding unit vectors $\mathbf{n}'$ and $\mathbf{h}'$ at the second nematic-glass interface. In these local reference frames the electric fields can be written in the form :

$$\mathbf{E}^i = [E_e^i, E_o^i]\,; \quad \mathbf{E}^r = [E_e^r, E_o^r] \quad \text{and} \quad \mathbf{E}^t = [E_e^t, E_o^t]\,, \tag{2.10}$$

where the suffixes e and o stand for « extraordinary » and « ordinary », respectively. We easily find :

$$\mathbf{E}^t = \bar{\bar{T}}_t\,\mathbf{E}^i \quad \text{and} \quad \mathbf{E}^r = \bar{\bar{T}}_r\,\mathbf{E}^i\,, \tag{2.11}$$

with

$$\bar{\bar{T}}_t = \bar{\bar{T}}_g^2\,\bar{\bar{T}}_P\,\bar{\bar{T}}_g^1 \quad \text{and} \quad \bar{\bar{T}}_r = \bar{\bar{T}}_g^1\,\bar{\bar{T}}_R\,\bar{\bar{T}}_g^2\,\bar{\bar{R}}_{ga}\,\bar{\bar{T}}_g^2\,\bar{\bar{T}}_P\,\bar{\bar{T}}_g^1\,, \tag{2.12}$$

where $\bar{\bar{T}}_g^1 = \exp(ik_g d_1)\,\delta_{ij}$ and $\bar{\bar{T}}_g^2 = \exp(ik_g d_2)\,\delta_{ij}$ are the isotropic transmission matrices for the glass plates I and II, respectively, and $\bar{\bar{R}}_{ga} = R\delta_{ij}$ is the reflection matrix at the second glass-air interface ($z = z_2$). $k_g = 2\pi n_g/\lambda$ is the wavenumber in the glass plates, n_g is the glass refractive index, $R = (n_g - 1)/(n_g + 1)$ is the reflection coefficient at the glass-air interface, and δ_{ij} is the Kronecher tensor. After simple calculations we find :

$$\bar{\bar{T}}_t = \begin{vmatrix} \exp(i\,\delta_e) & i\,[a\exp(i\,\delta_e) + b\exp(i\,\delta_o)] \\ i\,[b\exp(i\,\delta_e) + a\exp(i\,\delta_o)] & \exp(i\,\delta_o) \end{vmatrix} \tag{2.13}$$

and

$$\bar{\bar{T}}_r = R\begin{vmatrix} \exp(i\,2\,\delta_e) & R_{ab} \\ R_{ba} & \exp(i\,2\,\delta_o) \end{vmatrix}\,, \tag{2.14}$$

where

$$R_{ab} = i\,[a(\exp(i\ 2\ \delta_e) + \exp(i\ 2\ \delta_o)) + 2\,b\exp[i\,(\delta_o + \delta_e)]]\,, \tag{2.14'}$$

$$R_{ba} = i\,[b(\exp(i\ 2\ \delta_e) + \exp(i\ 2\ \delta_o)) + 2\,a\exp[i\,(\delta_o + \delta_e)]]\,, \tag{2.14''}$$

and $\delta_e = k_e\,d + k_g(d_1 + d_2)$, $\delta_o = k_o\,d + k_g(d_1 + d_2)$ are the optical dephasing of the extraordinary and ordinary waves, respectively. Equation (2.14) has been written by disregarding contributions of the second order in the small parameters a and b.

From (2.13) and (2.11) $\mathbf{E}^t$ writes as :

$$\mathbf{E}^t = \mathbf{t}'_e \exp(i\,\delta_e) + \mathbf{t}'_o \exp(i\,\delta_o)\,, \tag{2.15}$$

with

$$\mathbf{t}'_e = (E^t_e + iaE^t_o)\,\mathbf{n}' + ibE^t_e\,\mathbf{h}' \tag{2.16}$$

and

$$\mathbf{t}'_o = (E^t_o + iaE^t_e)\,\mathbf{h}' + ibE^t_o\,\mathbf{n}' \tag{2.17}$$

The transmitted electromagnetic wave of equation (2.15) can be interpreted as the superposition of two waves which propagate in the NLC layer with the phase velocity of the extraordinary and ordinary beams, respectively. For $a = 0$ and $b = 0$ (zero-th order approximation) these two waves are polarized parallel and orthogonal to the *local* director axis, thus, recovering the well-known result of the Adiabatic Theorem for slowly twisting NLC layers. For $a \neq 0$ and $b \neq 0$ (first-order approximation) the Adiabatic Theorem is no longer satisfied and the polarization of the « effective » extraordinary and ordinary waves do not coincide with the orientations of $\mathbf{n}'$ and $\mathbf{h}'$. From (2.14) and (2.11) $\mathbf{E}^r$ writes as :

$$\mathbf{E}^r = R\mathbf{t}_e \exp(i\ 2\ \delta_e) + R\mathbf{t}_o \exp(i\ 2\ \delta_o) + \mathbf{t}_A \exp[i\,(\delta_e + \delta_o)]\,, \tag{2.18}$$

with

$$\mathbf{t}_A = iR(a + b)(E^t_o\,\mathbf{n} + E^t_e\,\mathbf{h})\,, \tag{2.19}$$

where $\mathbf{t}_e$ and $\mathbf{t}_o$ are given by (2.16) and (2.17) with $\mathbf{n}$ and $\mathbf{h}$ in the place of $\mathbf{n}'$ and $\mathbf{h}'$. The first two terms in (2.18) correspond to two electromagnetic waves which propagate forward and backward in the NLC layer with the extraordinary and the ordinary wavenumber. The third component corresponds to the non-adiabatic electromagnetic wave which propagates with the average wavenumber $k_A = (n_e + n_o)\,k/2$.

2.2 TRANSMISSION AND REFLECTION FROM A NLC WEDGE. — Subsection 2.1 dealt with the case of a planar NLC layer sandwiched between two glass plane plates. Here we extend our analysis to the case of a NLC wedge sandwiched between two wedge glass plates as shown in figure 2. γ_n is the wedge angle of the NLC and γ_1 and γ_2 are the wedge angles of the glass plates I and II, respectively. If $\gamma_n \ll 1$, $\gamma_1 \ll 1$ and $\gamma_2 \ll 1$ the propagation of the electromagnetic wave in the NLC is still given by (2.18) with δ_e and δ_o linear functions of the x- co-ordinate (see Fig. 2). In particular :

$$\delta_e = (n_e\,d + n_g\,d_1 + n_g\,d_2)\,k - (n_e\,\gamma_n + n_g\,\gamma_1 + n_g\,\gamma_2)\,kx \tag{2.20}$$

and

$$\delta_o = (n_o\,d + n_g\,d_1 + n_g\,d_2)\,k - (n_o\,\gamma_n + n_g\,\gamma_1 + n_g\,\gamma_2)\,kx\,, \tag{2.21}$$

where k is the wavenumber of the incident beam, d is the thickness of the NLC at

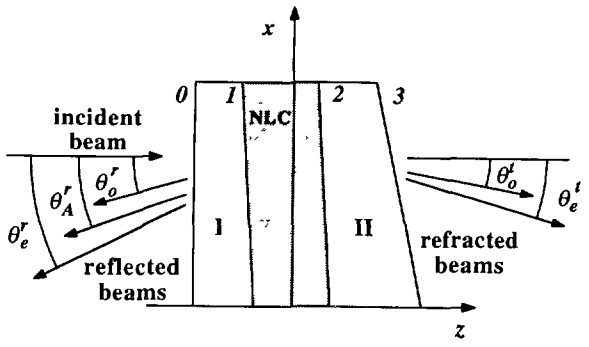

Fig. 2. — Geometry of the wedge nematic cell. The NLC wedge is sandwiched between two wedge glass plates I and II with wedge angles γ_1 and γ_2, respectively. The NLC makes a wedge angle γ_n. A twist of the director is present everywhere in the NLC sample. A monochromatic beam impinges at normal incidence on the first air-glass interface 0. Two different beams are refracted at the refraction angles θ_e^t and θ_o^t. The electromagnetic waves reflected by the glass-air interface 3 are separated by the wedge into three different reflected beams at the angles θ_o^r, θ_A^r and θ_e^r.

$x = 0$, d_1 and d_2 are the glass plate thicknesses at $x = 0$. In order to find the direction of the electromagnetic waves transmitted by the wedge, we make use of Fourier Optics [19]. On the basis of this theoretical procedure, we find that the two electromagnetic waves of (2.15) with the optical dephasings δ_e and δ_o given by equations (2.20) and (2.21) are refracted by the wedge at two different refraction angles θ_e^t and θ_o^t with respect to the incident beam :

$$\theta_e^t = [(n_e - 1)\,\gamma_n + (n_g - 1)\,\gamma_1 + (n_g - 1)\,\gamma_2] \tag{2.22}$$

and

$$\theta_o^t = [(n_o - 1)\,\gamma_n + (n_g - 1)\,\gamma_1 + (n_g - 1)\,\gamma_2]\,. \tag{2.23}$$

Therefore the angle between the two refracted beams is : $\Delta\theta = (n_e - n_o)\,\gamma_n$. The same Fourier analysis can be used to find the refracted beams that are generated by the electromagnetic field reflected by the second glass-air interface. In this case the electromagnetic field is made up of the superposition of three different waves (see Eq. (2.18)) which give three reflected beams. These beams make the following angles with respect to the beam reflected by the first air-glass interface :

$$\theta_e^r = [2\,n_e\,\gamma_n + 2\,n_g\,\gamma_1 + 2\,n_g\,\gamma_2]\,, \tag{2.24}$$

$$\theta_o^r = [2\,n_o\,\gamma_n + 2\,n_g\,\gamma_1 + 2\,n_g\,\gamma_2]\,, \tag{2.25}$$

and

$$\theta_A^r = [2\,n_A\,\gamma_n + 2\,n_g\,\gamma_1 + 2\,n_g\,\gamma_2]\,, \tag{2.26}$$

where $n_A = (n_e + n_o)/2$ is the average value between ordinary and extraordinary refractive indices of the NLC. By using equations (2.24), (2.25) and (2.26) we find the following relastionship between the three reflection angles :

$$\Delta\theta_{A-e}^r = \Delta\theta_{o-A}^r = \Delta\theta_{e-o}^r/2\,, \tag{2.27}$$

where $\Delta\theta_{A-e}^r = \theta_e^r - \theta_A^r$, $\Delta\theta_{o-A}^r = \theta_A^r - \theta_o^r$ and $\Delta\theta_{e-o}^r = \theta_e^r - \theta_o^r$. The non-adiabatic beam is reflected at exactly the average angle between the extraordinary and the ordinary beams. The amplitude and polarization of the non-adiabatic beam are given by (2.19). We want to point out

that our results have been obtained by neglecting losses due to reflections at various interfaces and light diffusion by the NLC. According to this approximation, the intensity of the non-adiabatic reflected beam is found to be independent of the incident beam polarization and is given by :

$$I_A^r = R^2(a+b)^2 I^i , \tag{2.28}$$

where I^i is the intensity of the incident beam. For an incident extraordinary (or ordinary) beam the polarization plane of the reflected non-adiabatic beam is orthogonal to that of the incident beam [see Eq. (2.19)].

As mentioned above our theorètical results have been obtained by assuming unitary transmission coefficients at the interfaces of different media. The transmission coefficients at the glass-NLC and NLC-glass interfaces are anisotropic. Therefore both the intensity and the polarization of the electromagnetic wave are expected to be slightly modified if the actual transmission coefficients are considered. Furthermore the average thickness of the NLC medium is somewhat high ($d \sim 100$ μm) in our experiment, hence diffusion from director fluctuations can contribute to both the intensity and the polarization of transmitted and reflected beams. All these effects are expected to give contributions of the order of 10 % to the amplitudes of the electromagnetic waves and, thus, equations (2.26), (2.27) and (2.28) are expected to be valid within this degree of approximation.

The above theoretical results allow a simple interpretation in terms of geometrical optics. Consider, for instance, an extraordinary optical beam which impinges on the NLC wedge. Due to the coupling between extraordinary and ordinary waves in the twisted NLC layer, the progressive optical beam propagates both as an extraordinary beam E which « sees » n_e and as an ordinary less intense non-adiabatic beam o which « sees » n_o. Capital and small letters indicate more intense and less intense beams, respectively. The two components E and o are refracted at different angles when crossing the NLC-glass interface 2 in figure 2. They are reflected by the glass-air interface 3 and, then, they are refracted further at the glass-NLC interface 2. Each of these two beams is, then, separated into an ordinary and an extraordinary component. Four different regressive waves propagate backward in the NLC wedge. The more intense beam EE is an electromagnetic wave which always propagates as an extraordinary wave ; this beam is, then, refracted at the same refraction angle for an extraordinary wave in a homogeneous planar wedge NLC. The component oO corresponds to a beam which is ordinary both during the forward and the backward propagation : this beam is refracted at the same angle as an ordinary beam in a homogeneous NLC wedge. Eo and oe represent waves in part ordinary and in part extraordinary during the propagation in the NLC. Eo is polarized at a right angle with respect to the extraordinary incident beam at the first air-glass interface, whereas oe has the same polarization plane of the incident beam. The amplitude of the latter beam is of the second order in the perturbation parameter thereby giving a negligible contribution. Both Eo and oe beams « see » the extraordinary refractive index for a half of the propagation length and the ordinary refractive index in the remaining part. Therefore the refraction angle of these two beams is intermediate between those of EE and oO beams.

2.3 STATIC AND DYNAMIC DIRECTOR DISTORTIONS IN AN ELECTRIC FIELD. — In this section we discuss the director-distortions in a NLC layer subjected to an electric field. Let us assume that a uniform electric field **E** is applied in the x-y plane along the x-axis and the easy director orientation $\mathbf{n}_0$ makes an angle β with **E**.

The total free energy is :

$$F = S\left\{\int_{-d/2}^{+d/2}\left[\frac{1}{2}K_{22}\,\varphi'^2 - \frac{\varepsilon_\alpha}{8\pi}E^2\cos^2(\beta-\varphi)\right]dz + W(\varphi_1) + W(\varphi_2)\right\} . \tag{2.29}$$

where the prime denotes differentiation with respect to z, K_{22} and ε_a are the twist elastic constant and the dielectric anisotropy of the NLC, S is the surface area and $W(\varphi)$ is the anchoring energy. In our experiment the director azimuthal angles at the two interfaces remain very close to the easy axes $\varphi_1 = \varphi_2 = 0$ and, thus, the anchoring energy can be written as :

$$W(\varphi) = \frac{1}{2} W_0 \varphi^2 \tag{2.30}$$

where W_0 is the azimuthal anchoring energy coefficient. Here we look for a uni-dimensional director distortion $\varphi(z)$. Due to the irrotational character of the electric field, $\partial E/\partial z = 0$ and, thus, $E(z) = \text{Cte}$. Therefore, by using the Euler-Lagrange variational procedure, we find that the director distortion which minimises equation (2.29) must satisfy :

$$\varphi'' - \frac{1}{2\xi^2} \sin [2(\beta - \varphi)] = 0 , \tag{2.31}$$

with the boundary conditions :

$$\varphi_1' = \frac{\varphi_1}{b} \quad \text{and} \quad \varphi_2' = -\frac{\varphi_2}{b} , \tag{2.32}$$

where we have defined the electric coherence length ξ and the extrapolation length b :

$$\xi = \frac{1}{E} \sqrt{\frac{4\pi K_{22}}{\varepsilon_a}} ; \quad b = \frac{K_{22}}{W_0} \tag{2.33}$$

If the electric field is much higher than the Frederiks threshold field ($\xi \ll d$), the first integral of equation (2.31) is :

$$\varphi' = \pm \frac{\sin(\beta - \varphi)}{\xi} \tag{2.34}$$

If $\beta > \varphi$, the signs + and − correspond to the sample regions $-d/2 < z < 0$ and $0 < z < d/2$, respectively. Therefore at the two interfaces of the NLC layer equations (2.8) are satisfied. By equating the left hand of equations (2.32) and (2.34), at the first order in the small angles φ_1 and φ_2 we obtain :

$$\varphi_1 = \varphi_2 = \sin(\beta) \frac{b}{\xi} \tag{2.35}$$

For small enough electric fields ($b \ll \xi$), $\varphi_1 = \varphi_2 \approx 0$ and, thus, φ' in equation (2.34) is a linear function of $1/\xi$. Therefore, according to equation (2.28), the intensity of the non-adiabatic beam is expected to be proportional to $1/\xi^2$.

The above theoretical results have been obtained by making the standard assumption that the elastic constant K_{22} has the same value everywhere in the NLC and that the interfacial behaviour can be entirely described by introducing a surface anchoring energy. In a thin interfacial layer close to the interface the former assumption is not completely satisfied since all physical parameters of the NLC are expected to become functions of the distance from the interface. Therefore the actual value of φ' at the interfaces can be different from that predicted by equation (2.34). However, far from the clearing point the thickness of the interfacial layer is expected to be about a few molecular lengths and, thus, much smaller than the optical wavelength. Under these conditions, by numerical integration of the Berreman electromagnetic equations, we find that the transmitted and reflected beams are practically insensitive to these short-range distortions and « see » only the macroscopic distortion which is given by equation

(2.34). This important point was the object of a detailed experimental check in a recent paper [17]. Therefore we can neglect all these subsurface elastic anomalies.

The theoretical results of this section apply to a static electric field by neglecting the effects of ionic electric charges. These latter effects can greatly affect the actual behaviour of the NLC by generating electrohydrodynamic instabilities. In practical experimental conditions the use of an a.c. electric field of a frequency higher than the relaxation frequency of charges in the NLC is convenient. As the ionic charges cannot follow the oscillations of the electric field, no electrohydrodynamic instabilities occur. The bulk electric torque acting on the director is proportional to the square power of the electric field and corresponds to the superposition of a static term proportional to the mean square of the electric field and of an oscillating second-harmonic contribution. If the period of the oscillating term is much higher than the characteristic reorientation time of the director, the director cannot follow the oscillating torque and a static distortion occurs everywhere. This static distortion can still be described by previous equations with the mean square root of the electric field E_{rms} in place of E.

In our experimental investigation we are also interested in analyzing the dynamic relaxation of the director distortion when the electric field is switched on. The director response time can be obtained by solving the Leslie-Ericksen hydrodynamic equations of NLC. A simple analytic expression of the relaxation time near the Frederiks threshold field E_{th} has been reported [23]. If $E \gg E_{th}$, the theoretical response time can be obtained by numerical integration of hydrodynamic equations. By using this numerical procedure, for $E > 10\,E_{th}$ we find that $\partial\varphi/\partial z$ approaches the stationary equilibrium value according to an exponential law with a characteristic time constant τ given by :

$$\tau = k\left[\frac{4\,\pi\gamma}{\varepsilon_\alpha E^2}\right], \tag{2.36}$$

where γ is the twist viscosity coefficient and $k = 1.01 \pm 0.01$ is a numerical coefficient virtually independent of the electric field intensity and of the angle between **n** and **E**. Figure 3 shows a typical time-dependence of $\partial\varphi/\partial z$ obtained by numerical integration. The exponential character of the relaxation curve near the equilibrium value is shown in the inset in a logarithmic scale. According to the theoretical analysis of subsection 2.2, the square root of the

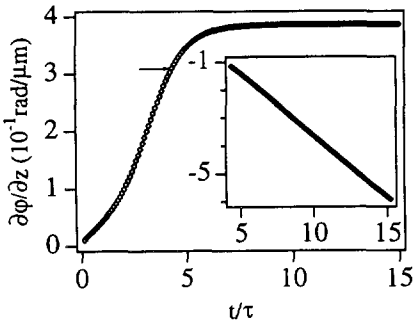

Fig. 3. — Theoretical behaviour of the normal derivative $\partial\varphi/\partial z$ at the nematic-glass interface *versus* the reduced time t/τ, where τ is given by (2.36). The NLC thickness is $d = 130$ μm and the electric field is $E = 16\,E_{th}$ where $E_{th} = \pi\,(4\,\pi K_{22}/\varepsilon_\alpha)^{1/2}/d$ is the Frederiks threshold field. The material parameters used to make numerical calculations are : $\varepsilon_\alpha = 11.8$, $K_{22} = 3.5 \times 10^{-7}$ dyne. The angle between the electric field and the easy axis is 86°. *Inset :* Logarithm of the difference between the normal derivative $\partial\varphi(t)/\partial z$ and its stationary value $\partial\varphi(\infty)/\partial z$ *versus* t/τ.

intensity of the non-adiabatic reflected beam is expected to be proportional to the surface derivative φ_1'. Therefore the characteristic relaxation time τ can be obtained from the measurement of the time-dependence of this intensity.

3. Experiment.

3.1 EXPERIMENTAL APPARATUS AND EXPERIMENTAL PROCEDURES. — In our experiment the bulk director twist is generated by an electric field **E** parallel to the average plane of the wedge. The geometry of the cell containing the NLC is shown in figure 4. The NLC is sandwiched between two wedge glass plates with wedge angles $\gamma_1 = \gamma_2 \approx 1°$. The NLC is 5CB (4-pentyl 4'-cyanobiphenyl) produced by BDH and exhibits a transition from the nematic to the isotropic phase at the clearing temperature $T_{NI} = 35.3$ °C. The surfaces of the two glass plates are covered by a thin (< 200 nm) film of PVA (Polyvinil Alchool) which is unidirectionally rubbed to induce a homogeneous planar alignment of **n** along $\mathbf{n}_0$ [20]. Two mylar stripes of different thicknesses (60 μm and 180 μm) are used as spacers to create a wedged NLC. Two parallel aluminium stripes of thickness 30 μm are inserted parallel to the wedge axis to generate the electric field. The two stripes are aligned at 5° with respect to $\mathbf{n}_0$, and their distance is $L = 5.3$ mm. An ac oscillating voltage is applied between the aluminium stripes in order to generate an electric field **E** lying in the plane of the NLC at the angle $\beta = 85°$ with $\mathbf{n}_0$. The amplitude of the oscillating voltage can be modulated by means of a signal generator. We use an AC electric field of period $T = 1$ ms in order to avoid charge injection from electrodes and electrohydrodynamic instabilities [18]. T is much shorter than the response time of the NLC in such a way that **n** cannot follow the electric field oscillation and a static $\mathbf{n}(z)$ distortion occurs everywhere. The **E** amplitude is chosen much higher than the threshold value for the Frederiks transition.

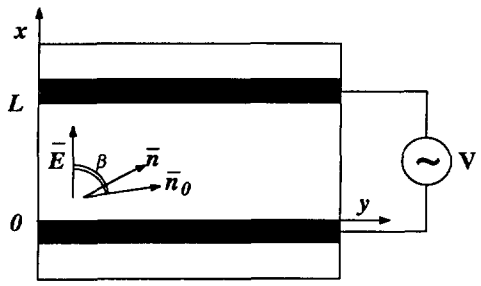

Fig. 4. — Schematic top view of the NLC experimental wedge cell. Two aluminium stripes are aligned parallel to the y-axis in such a way to generate an AC electric field **E** along the x-axis. $\mathbf{n}_0$ denotes the easy director axis at the two interfaces. **n** is the surface director when the electric field is switched on.

The experimental apparatus is schematically drawn in figure 5. The NLC cell is enclosed in a thermostatic box which ensures a temperature stability greater than 0.05 °C. A 5 mW He-Ne laser beam is polarized by a linear polarizer P and impinges at a virtually normal incidence on the NLC cell. The optical beams which are reflected by the second glass-air interface are collected by a photodiode Ph_1 which can be translated along two orthogonal axes by means of micrometric screws. An analyzer A can be inserted between the NLC wedge and Ph_1. A second photodiode Ph_2 collects the laser beam reflected by the first isotropic air-glass interface. The electric output signals of the two photodiodes are filtered by means of electronic

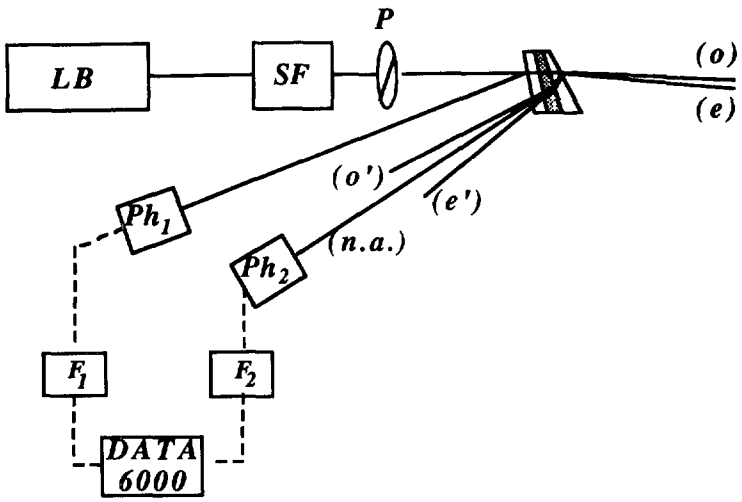

Fig. 5. — Schematic view of the experimental apparatus. LB = laser beam, SF = spatial filter, P = linear polarizer, o and e = transmitted nearly ordinary and extraordinary beams, o', e', n.a. = reflected beams from the second glass-air interface (3 in Fig. 1). o' and e' are the nearly ordinary and extraordinary beams, whilst n.a. is the non-adiabatic beam. Ph_1 and Ph_2 are linear photo detectors. F_1 and F_2 are electronic low pass filters.

analogic filters and then sent to two input channels of a signal digital analyzer (DATA 6100). The output of the photodiode Ph_1 is divided by that of the photodiode Ph_2 to eliminate spurious effects due to intensity fluctuations of the laser beam. The NLC cell is mounted on a micrometric two-axes translation stage to change in a continuous way the incidence point of the laser beam.

A possible spurious effect is the Joule heating due to the electric conductivity of the NLC. This effect can be detected by looking at the image of the NLC wedge in transmitted light between crossed polarizers. Due to the non-uniform thickness of the wedge, this image is characterized by a series of parallel interference fringes. Each interference fringe represents a region of the NLC where the optical dephasing $\Delta\varphi = 2\pi(n_e - n_o)d(x)/\lambda$ between the extraordinary and the ordinary waves has a constant value. A time-variation of NLC temperature produces a time-variation of the refractive indices and, hence, a continuous shift of the interference fringes. The sensitivity of this temperature measurement increases significantly if the initial NLC temperature is set very close to the clearing value T_{NI}. Indeed, the two refractive indices greatly change at a temperature close to T_{NI}. Since the refractive indices of the NLC 5CB are well-known [21], one can easily obtain the temperature variation of the NLC by measuring the shift of the interference lines. The measurement is performed by switching on the electric voltage and by measuring the phase shift *versus* time. As soon as **E** is switched on, the interference fringes show a very rapid displacement of the order of a fraction of the inter-fringe distance followed by a much slower displacement up to reaching a stationary pattern after a relaxation time of the order of 10 min. The initial rapid displacement (< 100 ms) is related to the optical effects due to the director distortion generated by **E** [17]. Therefore only the subsequent slow displacement is really related to temperature variations of the NLC. For the maximum value of the applied voltage ($V = 2\,800$ V rms) the temperature variation during the complete transient is $\Delta T = 1$ °C. With a suitable choice of the time duration of the electric field pulse we can reduce the variation of the NLC temperature to much less than 0.1 °C. All our experimental results have been obtained

under these conditions ; thus, the heating effects do not appreciably affect our experimental measurements.

In order to make a quantitative comparison between theory and experiment it is important to know the actual value of **E** in the incidence point $\mathbf{r} = (x, y)$ of the laser beam. In our experimental geometry, the amplitude of the electric field can be written in the general form :

$$E(\mathbf{r}) = \frac{V}{L} f(\mathbf{r}), \tag{3.1}$$

where $f(\mathbf{r})$ is a function of the frequency, the dielectric constants and the electric conductivity of the NLC, the dielectric constant of the glass plates and, finally, the geometric features of the wedge. As $f(\mathbf{r})$ cannot be calculated, we use a calibration procedure to obtain that. This calibration procedure exploits the time-dependence of the non-adiabatic beam at the switching on of the electric field. By modulating the ac voltage by a step function we find that the relaxation time is proportional to $1/E^2$ (see Fig. 8b) and, thus, the relative space variation of the electric field can be obtained by measuring this characteristic time in different points of the NLC sample. To increase the spatial resolution we focus the laser beam on a small region of the NLC (≈ 300 μm). Since $\tau \propto 1/E^2$, we find

$$E(\mathbf{r}) = \alpha / \sqrt{\tau(\mathbf{r})}, \tag{3.2}$$

where α is an unknown constant coefficient which can be obtained from the experimental values of $\tau(\mathbf{r})$ by exploiting the general condition :

$$V = \int_0^L E(x, y)\, dx = \alpha \int_0^L \frac{1}{\sqrt{\tau(x, y)}}\, dx, \tag{3.3}$$

The estimated error of the measurement of the local electric field is less than 5 %. Note that the electric field could be also obtained by exploiting the theoretical result of equation (2.36) and the measured value of the relaxation time. By substituting in equation (2.36) the measured value of the relaxation time and the known values of the constants γ [22] and ε_α [24], we calculate a local value of the electric field which agrees within the experimental accuracy with the results of the measurement above. The electric field is not uniform, it being greater when it is close to the two aluminium electrodes and becoming almost uniform in the central region of the cell. Due to the wedge shape of the NLC cell, the electric field amplitude reaches its minimum value in a point which is not exactly equidistant from the electrodes. All experimental measurements were performed setting the incidence point in the correspondence of the point of minimum electric field where the electric field gradients are negligible.

3.2 EXPERIMENTAL RESULTS. — According to the theoretical analysis of section 2, the propagation properties of a laser beam in the NLC wedge greatly depend on the angle θ made by the incident beam polarization with the director orientation at the first glass-nematic interface (1 in Fig. 1). The director orientation is expected to change according to equation (2.35) when the electric field is switched on. Therefore a direct measurement of φ_1 is needed to know the angle θ . φ_1 is measured by the intensity of the beam which is reflected by the first glass-nematic interface. According to reference [17], due to the anisotropy of the refractive indices of the NLC, the reflectivity coefficient at this interface depends on the value of the angle θ, being maximum when the polarization of the laser beam is parallel to the director. Therefore, the surface director angle can be obtained by rotating the polarizer P up to reach the maximum reflected intensity. In this way we can measure the director azimuthal angle with an uncertainty smaller than 0.1°. By repeating the measurement for different amplitudes of the

electric field and by exploiting equation (2.35) with ξ given in equation (2.33) we can obtain the experimental value of the extrapolation length b. At $T = 22$ °C we find $b = 0.1 \pm 0.01$ μm which corresponds to the anchoring energy coefficient $W_0 = (3.5 \pm 0.5) \times 10^{-2}$ erg/cm^2.

In the absence of the electric field, two different beams are reflected by the second glass-air interface (3 in Fig. 1) and two are transmitted by the NLC wedge. We easily verify that these beams correspond to ordinary and extraordinary optical beams. When the electric field is switched on, the intensity and the polarization of the transmitted and reflected beams show a variation due to breaking of the adiabatic theorem. In particular the polarizations of these beams do never correspond to the ordinary and extraordinary polarizations. Furthermore, as theoretically predicted, a new non-adiabatic reflected beam appears at a reflection angle intermediate between those of the extraordinary and ordinary beams. By translating the photodiode Ph_1 along an axis orthogonal to the wavevector of the non-adiabatic beam, we verify that the propagation vectors of the three reflected beams agree with the predictions of equation (2.27) within the experimental accuracy of ± 1 %. The intensity of the non-adiabatic beam is found to greatly increase as the amplitude of the electric field increases. For sufficiently small electric fields, the « non-adiabatic » beam is linearly polarized. In particular, if the incident beam is polarized along the director axis at the first nematic-glass interface (extraordinary polarization), the reflected beam is ordinary and the reverse holds for ordinary incident polarization. These polarization properties agree with the theoretical predictions of equation (2.19).

Figure 6 shows the intensity of the non-adiabatic reflected beam *versus* the angle θ made by the polarizer axis with the director at the first glass-nematic interface for a given value of the electric field. This intensity is not completely independent of the incident beam polarization but it shows a small variation (20 %) *versus* the θ-angle reaching the maximum value close to $\theta = 0$. The variation of the reflected intensity *versus* θ is not predicted by our theoretical formula (2.28). We note, however, that this effect is rather small and it cannot be ascribed to the effects of higher order contributions which were disregarded in equation (2.28). As a matter of fact, the same kind of intensity variation is found if the amplitude of the electric field is reduced to a half of its original value. We consider this variation as being caused by anisotropic loss of energy due to reflections at the two interfaces of the NLC and to light diffusion from the NLC. Both these effects were completely disregarded in our theoretical analysis. Note that, in our experimental conditions, the average thickness of the NLC sample is rather high and we can expect that light diffusion can affect the experimental results.

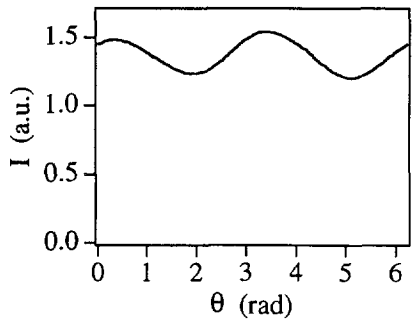

Fig. 6. — Intensity I of the non-adiabatic beam *versus* the angle θ between the polarization plane of the incident beam and the director orientation at the first glass-nematic interface. The rms value of the electric field is $E_{rms} = 3.25 \times 10^2$ V/cm. The vertical scale is in arbitrary units.

Figure 7 shows the intensity of the reflected non-adiabatic beam in arbitrary units *versus* $1/\xi^2$. The full line corresponds to the best linear fit of the experimental results below $1/\xi^2 = 10^7\ \text{cm}^{-2}$ In agreement with equation (2.28), for small enough electric fields ($\xi > 3\ \mu\text{m}$), the intensity of the non-adiabatic beam is proportional to $1/\xi^2$. For higher electric fields ($\xi < 3\ \mu\text{m}$), a deviation from linearity is observed. According to theoretical analysis in section 2, two different physical mechanisms can be responsible for this deviation : the effect of higher order contributions in the perturbative parameter $\varepsilon = 1/\Delta k\xi$ and the director displacement at the interfaces due to the finite anchoring energy (see Sect. 2.3). The latter contribution can be experimentally analysed by making a direct measurement of the surface director orientation *versus* the electric field. This allows us to obtain the experimental value of the parameters $A = [\sin(\beta - \varphi_1)/\xi]^2$ and $B = [\sin(\beta - \varphi_2)/\xi]^2$. Since both interfaces are treated in the same way we find $\varphi_1 \approx \varphi_2$ and $A = B$. According to equations (2.28) and (2.8), at the first order in ε, the intensity of the non-adiabatic beam should be proportional to A. In our experiment, the rotation of the director at the surface when the electric field has the maximum value is $\varphi_1 = 2.8 \pm 0.1°$ and $\sin(\beta - \varphi_1)$ varies from 0.996 to 0.991 at varying the electric field from 0 to its maximum value. This means that the contribution of finite anchoring to deviations from linearity *versus* $1/\xi^2$ in figure 7 is rather small ($\approx 1\ \%$). Therefore these deviations are mainly due to breaking of the first order formula of equation (2.28).

Figure 8a shows the characteristic time-response of the square root of the intensity I of the non-adiabatic beam to a step voltage. We easily verify that, after a transient time (≈ 0.5 s), the intensity exponentially approaches the stationary value according to the theoretical predictions of section 2.3.

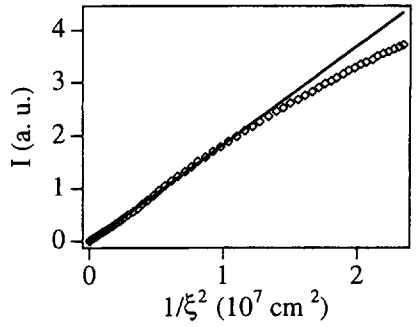

Fig. 7. — Intensity I of the non-adiabatic beam *versus* $1/\xi^2$ at the temperature $T = 23$ °C. ξ is obtained by (2.33) with the material parameters of 5CB $\varepsilon_\alpha = 11.8$ [24] and $K_{22} = 3.5 \times 10^{-7}$ dyne [25]. The full line is the best linear fit on the experimental points with $1/\xi^2 < 10^7\ \text{cm}^{-2}$ The intensity is in arbitrary units.

Figure 8b shows the director relaxation time τ *versus* ξ^2 at the temperature $T = 23$ °C. The time it is obtained by making the best fit of $(I)^{1/2}$ *versus* t with respect to an exponential law starting from the point where $(I)^{1/2}$ reaches 4/5 of the equilibrium value (see the arrow in Fig. 8a). The full line corresponds to the linear best fit of the experimental points. The angular coefficient of the straight line in figure 8b allows us to estimate the twist viscosity coefficient $\gamma = 1.02 \pm 0.1\ p$ exploiting equation (2.36) with $k = 1.01$ and ε_α and K_{22} taken from reference [24] and [25] respectively. The measured value of the twist viscosity coefficient agrees within the experimental uncertainty with the value $\gamma = 0.93 \pm 0.03\ p$ which is given in reference [22]. The rather large relative error of γ in our experiment is almost entirely due to the large uncertainty (5 %) of the electric field amplitude caused by the non-uniformity of the electric

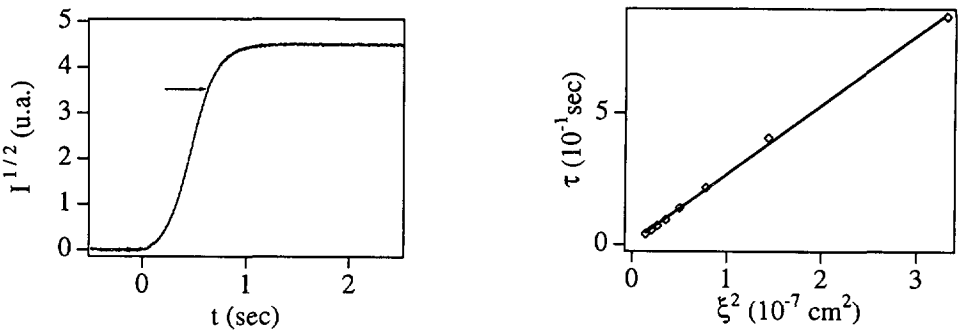

Fig. 8. — a) Typical experimental time-variation of $I^{1/2}$ when an electric field is switched on at the time $t = 0.05$ s. The characteristic relaxation time τ is obtained by making the best exponential fit of the experimental points starting from the arrow in figure. The vertical scale is in arbitrary units. b) Experimental relaxation time τ *versus* ξ^2. The full line denotes the best linear fit of the experimental points. ξ is calculated as discussed in figure 7.

field (see Sect. 3.1). This error could be greatly reduced by using a magnetic field in place of the electric field.

4. Conclusions.

In this paper we have shown that a very simple and general analytic expression can be obtained for an electromagnetic field of wavelength λ which propagates in a twisted NLC having a characteristic twist length $\xi \gg \lambda$. This expression has been utilised to explain the main features of the propagation and reflection of a laser beam by a twisted NLC wedge. Due to the breaking of the well-known adiabatic theorem, we have predicted the occurrence of a new beam reflected at an average angle between the extraordinary and the ordinary beam angles. The intensity of this reflected beam is found to depend only on the derivative of the director-field at the two interfaces of the NLC wedge and does not depend on details of the bulk director distortion. The study of the dynamic response of this beam to a step-like voltage provides a simple experimental method to measure the twist viscosity coefficient γ of NLC. The main theoretical predictions are in satisfactory agreement with the experimental results.

Acknowledgements.

We acknowledge the Ministero della Pubblica Istruzione (Italy) and the Consiglio Nazionale delle Ricerche (Italy) for financial support.

References

[1] Oseen C. W., *Trans. Faraday Soc.* **29** (1933) 833.
[2] De Vries H., *Acta Crystallogr.* **4** (1951) 219.
[3] Dreher R. and Meyer G., *Phys. Rev. A* **8** (1973) 1616.
[4] Belyakov V. A. and Dmitrienko V. D., *Sov. Phys. Solid State* **15** (1974) 1811.
[5] Belyakov V. A., Dmitrienko V. D. and Orlov V. P., *Sov. Phys. Usp.* **22** (1979) 63.
[6] Akopyan R. S., Zeldovich B. A. and Tabirian N. V., *Sov. Phys. JEPT* **56** (1982) 1024.
[7] Oldano C., *Phys. Rev. A* **31** (1985) 1014.

[8] Ong H. L., *Phys. Rev. A* **37** (1988) 3520.
[9] Allia P., Oldano C. and Trossi L., *Physica Scripta* **37** (1988) 755.
[10] Allia P., Oldano C. and Trossi L., *Mol. Cryst Liq. Cryst.* **143** (1987) 17.
[11] Allia P., Oldano C. and Trossi L., *J. Opt. Soc. Am. B* **3** (1986) 424.
[12] Berreman D. W., *J. Opt. Soc Am.* **62** (1972) 502.
[13] Berreman D. W., *Mol. Cryst. Liq Cryst.* **22** (1973) 175.
[14] Ong H. L., *Phys. Rev. A* **32** (1985) 1098.
[15] Ong H. L. and Meyer R. B., *J. Opt. Soc. Am.* **2** (1985) 168.
[16] Barbero G., Miraldi E., Oldano C., Rastrello M. L. and Taverna Valabrega P., *J. Phys. France* **47** (1986) 141.
[17] Faetti S. and Lazzeri C., *J. Appl. Phys.* **71** (1992) 3204.
[18] See, for instance, de Gennes P. G., The Physics of Liquid Crystals (Clarendon Press, Oxford, 1974).
[19] Goodman J. W., Introduction to Fourier Optic (Mc Graw-Hill New York, 1968).
[20] Cognard J., *Mol. Cryst. Liq. Cryst. Suppl.* **1** (1982) 1.
[21] Karat P. P. and Madhusudana N. V., *Mol. Cryst. Liq. Cryst.* **36** (1976) 51.
[22] Coles H. J. and Sefton M. S., *Mol. Cryst. Liq. Cryst. Lett.* **1** (1985) 151.
[23] Pieransky P., Brochard F. and Guyon E., *J. Phys. France* **33** (1972) 681 and **34** (1973) 35.
[24] Ratna B. R. and Shashidhar P., *Mol. Cryst. Liq Cryst.* **42** (1977) 113.
[25] Faetti S., Gatti M. and Palleschi V., *J. Phys. France Lett.* **46** (1985) 881.